

Nonlinear Optical Effects in Photonic Crystals

Xiang He
Department of Electrical and Computer Engineering
University of New Mexico

Abstract

In the past few years, the nonlinear optical effects in the photonic crystals have attracted significant attention because these effects can be used to make many optics devices in many different fields. In this paper, background knowledge about photonic crystals is firstly introduced. Then I summarized the applications using nonlinear optical effects in photonic crystals. I also introduced an Au coaxial aperture array built on the GaAs substrate which was proved to achieve SHG based on a different mechanism.

Key Words: nonlinear optics effects, photonic crystal

Introduction of photonics

Photonic crystals are composed of periodic dielectric or metal-dielectric nano-1D, 2D or 3D structures as shown in the figure 1 below, depending on the specific applications. It's usually viewed as an optical analog of semiconductors that modify the properties of light similarly to a microscopic atomic lattice. Photonic crystals are designed on purpose to affect the propagation of electro-magnetic waves (EMW) in the same way as the periodic potential in a semi-conductor crystal affects the electron motion by defining allowed and forbidden electronic energy bands. The absence of allowed propagating EM modes inside the structures, corresponding to a range of the wavelengths called a photonic band gap, gives rise to the distinct optical phenomena such as inhibition of spontaneous emission¹, high-reflection omnidirectional mirrors and low-loss-waveguiding amongst others. Since the basic physical phenomenon is based on diffraction, the periodicity of the photonic crystal structure has to be in the same length-scale as roughly half the wavelength of the EM waves.

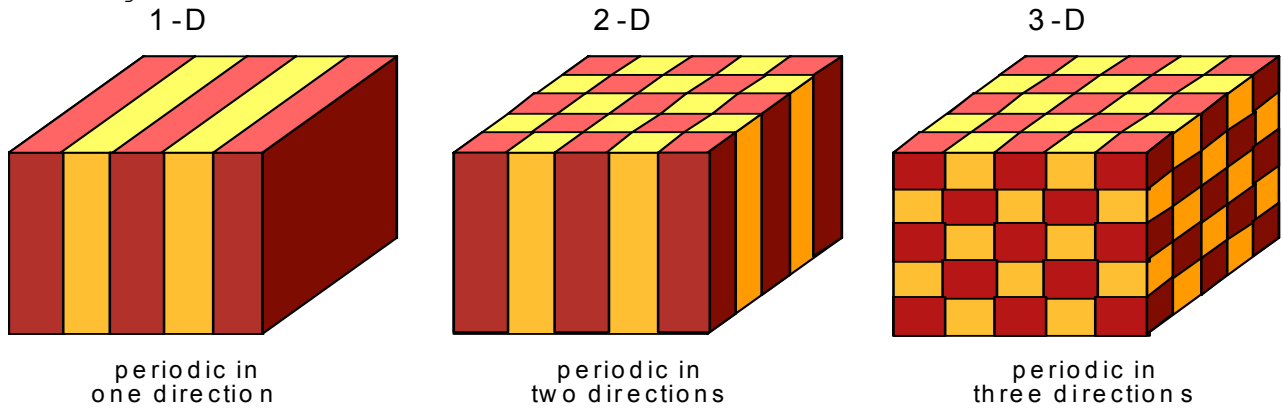


Figure 1. Schematics of 1D, 2D, 3D photonic band gap materials(photonic crystal)

Nonlinear Optics Effects of Photonics Crystal

NLO Effects With Defects

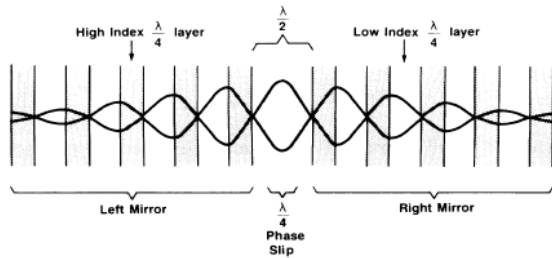


Figure 2.

A 1D defect of $\lambda/2$ thick inserted in a 1D photonic crystal consist of periodic $\lambda/4$ phase slip. Those $\lambda/4$ phase slips on the left and right sides of $\lambda/2$ defect layer will act as high reflection mirrors. And the $\lambda/2$ layer will behave like a Fabry-Perot resonator.

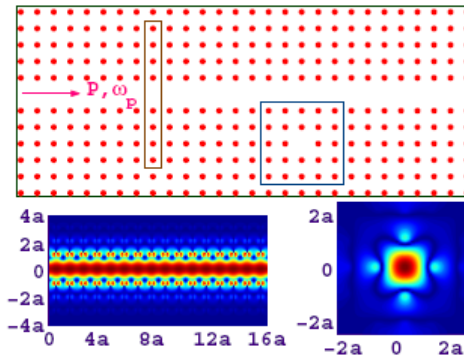


Figure 3.

Schematics of a 1D and 0D defects in a 2D PhC with square symmetry (a is the lattice pitch). The two rectangles represent the super-cells used to find the defect modes and corresponding mode frequencies. In the low panels, the electric field (TM polarization) of the 0D cavity mode (right) and 1D waveguide mode (left).

Photonic crystals (PhCs) are expected to play an important role in the development of new optical devices. The devices possibilities for PhCs will be greatly enhanced by the addition of optical nonlinearities; such possibilities include ultra-fast all-optical switching for communications, and potentially even optical computing²⁻⁷.

Usually, those researches about the enhancement of nonlinear optics in PhCs are based on the different types of structural defects. In the 1D PhCs with defect, people observed a large enhancement of degenerate four-wave mixing efficiency⁸. Since the total thickness of the whole structure is only a few micrometers, it was successfully used to form an optical phase-conjugated image. Similarly, if you fill the defects in 1D PhCs with nonlinear organic dye, you can perform nonlinear spectroscopy⁹ around the defect resonance and at frequencies well away from resonance. In those 2D or 3D PhCs, we may have point-like or linear defects. The linear defects in PhCs can act as efficient waveguides, transmitting light around sharp corners with relatively small losses^{10,11}. Furthermore, under certain circumstances, point-like defects in PhCs can localize the electromagnetic energy near the defect for certain frequencies that are forbidden to propagate within the bulk of PhCs, enabling the creation of micro-cavity resonators that can be used to efficiently couple light into PhC-based waveguides. This effect can be used to design resonant add-drop filters¹², and other integrated optical components¹³⁻¹⁷. Potentially, these applications can lead to the design of new compact integrated optoelectronic or all-optical circuits.

NLO Effects Without Defects

We can also make a special structure with specific nonlinear material to achieve nonlinear optics effects without intentionally making defects. The former graduate student in my group, Wenjun Fan made the subwavelength coaxial metallic aperture array on GaAs substrate has been proved to enhance obviously the second harmonic generation¹⁸ (SHG). The specialty and an important merit of this subwavelength coaxial metallic aperture array is enhanced electromagnetic fields concentrating at the coax gap area associated with enhanced transmission, which in turn can be used to enhance second harmonic generation. A nano-scale coaxial metallic aperture array was fabricated with an isotropic nonlinear material (GaAs) in the coaxial gap region. SHG was experimentally realized in this kind of structure with an optical path length $\ll \lambda$, so that the phase matching is not required. This is the first demonstration of SHG from a material with a non-zero second-order susceptibility ($\chi^{(2)} > 0$) using nano-photonic metal array.

The figure 4 on the next page shows the whole procedure of making this 2D photonic Crystal. Since fabrication of this structure is not this paper's intent to introduce, we will not go through the detail about the processing flow. The square-array pitch was 720 nm in orthogonal directions on the surface, with coaxial inner radius of 114 nm an outer radius of 199 nm (gap width 85 nm). The metal film was e-beam evaporated with 5nm Ti layer for adhesion underneath the 70nm thick Au layer. The height of GaAs annulus was 140nm, so the GaAs extends above the metal film.

Basic Knowledge of SHG

For a second harmonic generation material with susceptibility $\chi^{(2)}$, assuming the depletion of the fundamental wave at frequency ω is negligible as it's converted to 2ω after passing through the NLO material of length L , the output power at the second harmonic can be given by the formula below

$$E^{(2\omega)}(L)E^{(2\omega)*}(L) = \left(\frac{\mu_0}{\epsilon_0}\right) \frac{\omega^2(\chi^{(2)})^2}{n^2(\omega)} L^2 |E^{(\omega)}|^4 \frac{\sin^2\left(\frac{\Delta kL}{2}\right)}{\left(\frac{\Delta kL}{2}\right)^2} \quad (1)$$

Where $\Delta k = k^{(2\omega)} - 2k^{(\omega)}$, $n^2 = \epsilon/\epsilon_0$. The SH output power gets his maximum at $\Delta kL/2=0$, and has zeros when $\Delta k/L = m\pi$ ($m=1, 2, 3\dots$). A coherence length can be defined by the distance between the maximum peak and the first minima as $L_c = \pi/\Delta k$. The intensity which is power per unit area then is given as

$$I^{(2\omega)} = \frac{P^{(2\omega)}}{A} = \frac{1}{2} \sqrt{\frac{\epsilon^{(2\omega)}}{\mu_0}} |E^{(2\omega)}|^2 \quad (2)$$

The coherence length is essentially a measure of the maximum useful crystal length. Traditional phase matching methods involve birefringent angle tuning or temperature-tuning a NLO crystal according to the refractive index ellipsoids to achieve $\Delta k=0$. Another way to get significant SH growth is to use quasi-phase matching (QPM) which is to modulate the nonlinear susceptibility with a period that matches the coherence length in the nonlinear medium, as was described theoretically by Armstrong¹⁹ et al.

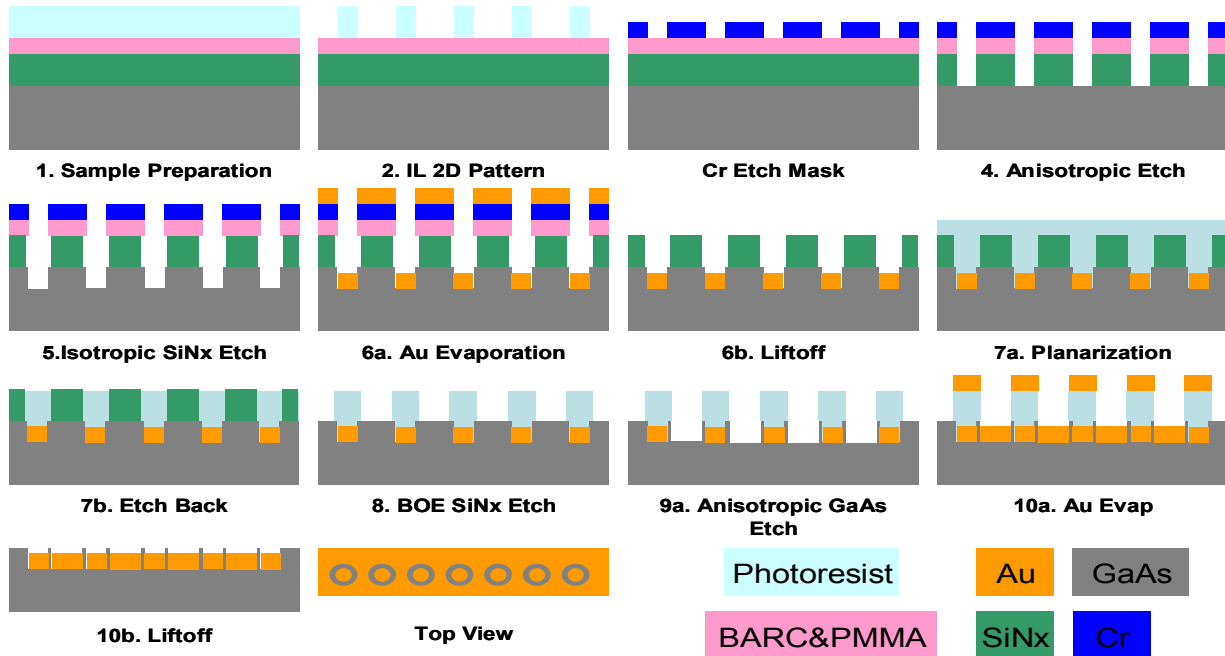


Figure4. Processing flow for metallic coaxial array on GaAs substrate

GaAs, a well known isotropic semiconductor, which has high second-order susceptibility, broad transparency range 0.9-1.7 μm , low absorption and high thermal conductivity. As a result of its optical isotropy, no birefringence is displayed. Thus, it's not phasemathcable. Epitaxial grown orientation-patterned GaAs was developed to introduce QPM for nonlinear applications, along with random QPM in polycrystalline isotropic nonlinear materials and artificial birefringence of multilayer composites of GaAs and AlAs.

But the method we used to achieve high nonlinear effect in single crystalline GaAs is based on another aspect of SHG, where the SH intensity is proportional to the 4th power of the optical field of the fundamental pump light as shown

equations (1) and (2). Wenjun Fan applied subwavelength metallic coaxial structure on the GaAs substrate with GaAs in between the center metal island and the surrounding metal webbing of the coaxial aperture. Thus, high electrical field, resulting from the transmission of the localized resonant mode (coax TE₁₁ mode) and delocalized surface plasmon modes at the fundamental pump wavelength, concentrated in the patterned GaAs with high second order susceptibility, magnified the SH intensity by 4th power of the electrical field enhancement factor. Since the GaAs thickness is much shorter than the (fundamental, SH) wavelengths involved here and thus much shorter than the coherence length, no phase matching is needed to enhance the SH signal from this very thin structure.

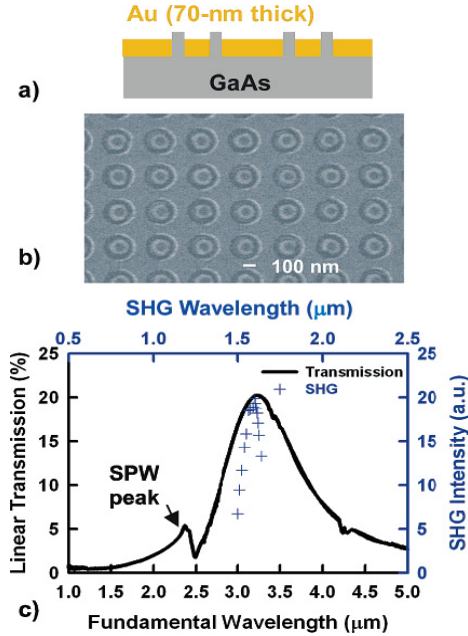


Figure 5.
 (a) Schematic cross section of structure showing GaAs annuli protruding through the Au film.
 (b) Top down SEM of fabricated structure.
 (c) FTIR linear transmission spectrum and wavelength-dependent SHG signal spectrum.

a short-pass filter with a cutoff at 2.0 μm and a monochromator and was detected with an InGaAs photoreceiver using a lock-in amplifier.

To quantify the conversion efficiency, Wenjun Fan compared the normal incidence SH signal from the nanopatterned coaxial GaAs sample with that from a Z-cut LiNbO₃ wafer at a fundamental pump wavelength of 3.23 μm, as shown in figure 6. The SHG radiation intensity for both samples scales as the square of the fundamental intensity. The SH signal for Z-cut LiNbO₃ is about 72 times larger than that from the GaAs sample. After factoring in the difference of the reflection of the fundamental pump intensity in the front surface [$R_{\text{LiNbO}_3}(\omega) \cong 13\%$ and $R_{\text{GaAs}}(\omega) \cong 29\%$] and that of SH intensity in the back patterned surface [$R_{\text{LiNbO}_3}(2\omega) \cong 14\%$ and $R_{\text{GaAs}}(2\omega) \cong 29\%$] as well as the available SH signal generation area (only 16% of the sample area is not covered by metal), the ratio of the signal is reduced to 9.4, that is, the GaAs SHG signal is 0.11 times as intense

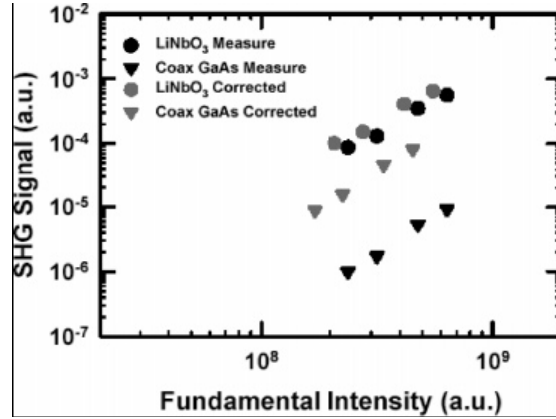


Figure 6.
 SH intensity versus fundamental intensity for Z-cut LiNbO₃ and coaxial patterned GaAs at a fundamental wavelength of 3.23 μm. The curve labeled “corrected” are adjusted for Fresnel reflectivities and the GaAs open area.

An IR-OPA, producing optical pulses with 200-fs duration and 15-nm band width at 1k Hz repetition rate, was used as the pump source for SHG. The unfocused laser output beam with a diameter of 1.0mm passed through a chopper and a long-pass filter with a cutoff at 2.5 μm, and was directed at normal incidence onto the unpatterned side of the sample. The transmitted light which contained both the fundamental pump wavelength and the SH radiation, passed through

as that from the Z-cut LiNbO₃. The second-order nonlinear coefficients calculated using Miller's rule are $d_{14} \cong 87 \text{ pm/V}$ for GaAs and $d_{31} \cong 4 \text{ pm/V}$ for LiNbO₃ at this wavelength. However, the spatial extent of the nonlinear generation is only about 140nm for nanopatterned GaAs compared with a coherence length of 14 μm for LiNbO₃ at this wavelength.

Summary

In this paper, I introduced background knowledge about what photonic crystal is and the progresses of the nonlinear optical effects in photonic crystals made by people in the past few years. The potential applications were also mentioned. Additionally, a different way to generate SH proved by one of my group's former students Wenjun Fan was also introduced in a bit more detail.

Reference

- [1] Inhibited Spontaneous Emission in Solid-State Physics and Electronics, Eli Yablonovitch, Phys.Rev. Lett. 58, 2059 (1987).
- [2] M. Scalora, J. P. Dowling, C. M. Bowden, and M. J. Bloemer, Phys. Rev. Lett. 73, 1368 (1994)
- [3] S. John and T. Quang, Phys. Rev. A 54, 4479 (1996)
- [4] P. Tran, Opt. Lett. 21, 1138 (1996)
- [5] A. Forchel, Nat. Mater. 2, 13 (2003)
- [6] M. Soljagic, M. Ibanescu, S. G. Johnson, Y. Fink, and J. D. Joannopoulos, Phys. Rev. E 66, 055601 (2002)
- [7] A. Huttunen and P. Torma, J. Appl. Phys. 91, 3998 (2002)
- [8] Noriaki Tsurumachi, Shoichi Yamashita, norio Muroi, Takao Fuji, Toshiaki Hattori and Hiroki Nakatsuka, J. Appl. Phys. 88, 6302 (1999)
- [9] Garrett, J. Schneider and George H. Watson, Appl. Phys. Lett. 83, 5350 (2003)
- [10] A. Mekis, J.C. Chen, I. Kurland, S. Fan, P. R. Villeneuve, and J. D. Joannopoulos, Phys. Rev. B 59, 4809(1998)
- [11] S. Y. Lin, E. Chow, V. Hietala, P. R. Villeneuve, and J. D. Joannopoulos, Science 282, 274(1998)
- [12] S. Fan, P. R. Villeneuve, J. D. Joannopoulos, and H. A. Haus, Phys. Rev. Lett. 80, 960(1998); S. Fan, P. R. Villeneuve, J. D. Joannopoulos, M. J. Khan, C. Manolatu, and H. A. Haus, Phys.Rev.B 59, 15882(1999).; Nicolae C. Panoiu, Mayank Bahl, and Richard M. Osgood, Jr., Optics Express Vol12, No8, 1605 (2004)
- [13] M. J. Steel, M. Levy, and R. M. Osgood, IEEE photonics Technol. Lett. 12, 1171 (2000).
- [14] M. J. Steel, M. Levy, and R. M. Osgood, J. Lightwave Technol. 18, 1289,(2000);18, 1297 (2000).
- [15] J. P. Dowling, M. Scalora, M. J. Bloemer, and C. M. Bowden, J. Appl. Phys. 75, 1896 (1994).
- [16] S. G. Johnson, C. Manolatu, S. Fan, P. R. Villeneuve, J. D. Joannopoulos, and H. A. Haus, Opt. Lett. 23, 1855 (1998).
- [17] B. D'Urso, O. Painter, J. O'Brian, T. Tombrello, A. Yariv, and A. Scherer, J. Opt. Soc. Am. B 15, 1155(1998);O. Painter, J. Vuckovic, and A. Scherer, ibid, 16,275 (1999).
- [18] Wenjun Fan, Shuang Zhang, N. C. Panoiu, A. Abdenour, S. Krishna, R. M. Osgood, Jr., K. J. Malloy, And S. R. J. Brueck, Nano Letters, Vol.6, No.5,1027 (2006)
- [19] J. A. Armstrong, N. Bloembergen, J. Ducuing, and P. S. Pershan, "Interactions between light waves in a nonlinear dielectric", Phys. Rev. 127, 1918 (1962)